Nonlinear Control of Heartbeat Models

Witt THANOM
Robert N. K. LOH

Department of Electrical and Computer Engineering
Center for Robotics and Advanced Automation
Oakland University
Rochester, Michigan 48309, U. S. A.

ABSTRACT

This paper presents a novel application of nonlinear control theory to heartbeat models. Existing heartbeat models are investigated and modified by incorporating the control input as a pacemaker to provide the control channel. A nonlinear feedback linearization technique is applied to force the output of the systems to generate artificial electrocardiogram (ECG) signal using discrete data as the reference inputs. The synthetic ECG may serve as a flexible signal source to assess the effectiveness of a diagnostic ECG signal-processing device.

Keywords: Heartbeat model, Electrocardiogram, Nonlinear control, Feedback linearization, Phase portrait analysis.

1. INTRODUCTION

The human heart is a complex and yet robust system. One of the most important signals that relates to human heart operation is the ECG signal. It is a time-varying signal representing the electrical potential generated by the electrical activity in the cardiac tissue. A single cycle of the ECG reflects the contraction and relaxation of the heart, leading to the heart's pumping action. The ECG can be measured by recording the potential between two electrodes placed on the surface of the skin at some pre-determined points. Characteristic information extracted from the ECG signal can be used to indicate the state of cardiac health as well as a potential heart problem [1].

Much effort has been invested into the development of mathematical models that describe the operation of the human heart. One of the crucial developments is by Zeeman [2], where he developed a mathematical model that captured three important qualities of cardiac characteristics: (i) stable equilibrium; (ii) threshold for triggering an action potential; and (iii) return to equilibrium. The resulting models are a 2^{nd}-order nonlinear differential equation representing the heartbeat system, and a 3^{rd}-order nonlinear differential equation that can be applied to the nerve impulse. Other interesting and related models were presented in [3 - 6].

Research that focuses on generating the ECG signal is also very active. In [7], the 3-dimensional nonlinear model from [2] was modified by adding a control variable in order to control the heart rate variability and to produce the ECG using a neural network. In [8], the authors modified the 2^{nd}-order nonlinear heartbeat system in [2] by adding an on-off type control variable representing the pacemaker for fulfilling the mechanism of contraction-relaxation of the heart. In [9], a dynamical model that generates a synthetic ECG signal by specifying the mean and the standard deviation of the heart rate and the power spectrum of the RR tachogram was proposed. The model does not address how the heart works but rather utilizes the statistical information of the ECG as *a priori* data to generate a signal.

This paper presents a novel application of nonlinear control system theory – feedback linearization – to the heartbeat systems originated from [2]. The systems were modified by adding a pacemaker to provide the control channel. One of the objectives is to create a synthetic ECG signal based on existing ECG data, where the data is used as the reference signal for a tracking control problem. The synthetic ECG signal can be used as a flexible signal source to assess the effectiveness of a diagnostic ECG signal-processing device [7]. The paper is organized as follows. In Section 2, the model dynamics and its characteristics are investigated. Phase portrait and stability analysis are conducted. The nonlinear feedback linearization control theory is developed in Section 3, and applied to the heartbeat systems to create a synthetic ECG in Section 4. Lastly, the conclusion is presented in Section 5.

2. HEARTBEAT MATHEMATICAL MODELS

There are two states of the heart in a cycle of the heartbeat: *diastole* which is the relaxed state, and *systole* which is the contracted state. The cycle starts when the heart is in the diastolic state. The pacemaker which is located at the top of the right atrium – one of the upper chambers of the heart – triggers an electrochemical wave that spreads slowly over the atrium. This electrochemical wave causes the muscle fibers to contract and push the blood into the ventricles – the lower chambers of the heart. The same electrochemical wave then spreads rapidly over the ventricles causing the whole ventricle to contract into the systolic state, and pumping the blood into the lung and the arteries. Immediately following the systolic state, the muscle fibers quickly relax and return the heart to the diastolic state to complete one cycle of the heartbeat [8].

Second-Order Nonlinear Heartbeat Model

A mathematical model that describes the behavior of the heartbeat was developed in [2], where it was suggested that such a model should contain three basic features:

(i) a stable equilibrium state representing diastole;
(ii) the threshold for triggering the electrochemical wave causing the heart to go into systole; and
(iii) the return of the heart into the diastolic state.

The resulting model is given by

$$\varepsilon \dot{x}_1 = -\left(x_1^3 - Tx_1 + x_2\right), \qquad T > 0, \tag{1}$$

$$\dot{x}_2 = x_1 - x_d\,, \tag{2}$$

where $x_1(t)$ represents the length of the muscle fiber, $x_2(t)$ is a variable related to electrochemical activity; the parameter ε is a small positive constant associated with the fast eigenvalue of the system, x_d is a scalar quantity representing a typical length of muscle fiber in the diastolic state, and T represents tension in the muscle fiber. Fig. 1 illustrates the phase portrait of Eqs. (1) and (2) with the initial conditions along the left and right diagonals across the $x_1 - x_2$ plane. The parameter values used to produce the phase portrait are $\varepsilon = 0.2$, $T = 1$, and $x_d = 0$.

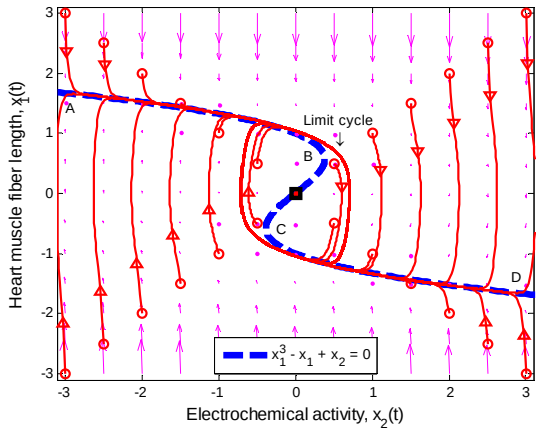

Figure 1. Phase portrait of the 2nd-order heartbeat system.

In Fig. 1, the cubic line (dashed curve) represents the steady-state of Eq. (1). When $x_d = 0$ in Eq. (2), the equilibrium point of the system is at the origin. All trajectories initiated above the cubic line, that is, $x_1^3 - Tx_1 + x_2 > 0$, direct downward toward the origin along the cubic line. Likewise, all trajectories started below the cubic line, i.e., $x_1^3 - Tx_1 + x_2 < 0$, direct upward toward the origin along the cubic line. All trajectories end up at the limit cycle around the equilibrium point. It is obvious that the equilibrium point is unstable as the vector field inside the limit cycle directs away from the point. This conclusion can be confirmed by analyzing the stability of the equilibrium point using the well-known Lyapunov indirect stability theorem [10]. For this purpose, let **A** be the constant Jacobian matrix of Eqs. (1) and (2) at the origin, it follows that

$$\mathbf{A} = \left.\frac{\partial \mathbf{f}(\mathbf{x})}{\partial \mathbf{x}}\right|_{\mathbf{x}=\mathbf{0}} = \begin{bmatrix} -\frac{1}{\varepsilon}\left(3x_1^2 - T\right) & -\frac{1}{\varepsilon} \\ 1 & 0 \end{bmatrix}_{\mathbf{x}=\mathbf{0}} = \begin{bmatrix} \frac{T}{\varepsilon} & -\frac{1}{\varepsilon} \\ 1 & 0 \end{bmatrix}, \tag{3}$$

where $\mathbf{f}(\mathbf{x}) = \begin{bmatrix} \frac{-1}{\varepsilon}\left(x_1^3 - Tx_1 + x_2\right) & x_1 - x_d \end{bmatrix}^T$.

The eigenvalues of **A** are given by $\lambda_1 = 3.62$ and $\lambda_2 = 1.38$ for $T = 1$ and $\varepsilon = 0.2$. Therefore, the origin is unstable since both eigenvalues are real and positive.

In Fig. 1, since the vector field around the segment AB and CD always points toward the cubic line, and away from the cubic line in the BC portion, any point along the cubic line in the AB and CD segments is considered to be stable whereas points along the BC section are unstable. The points B and C are important as they specify the *threshold* – the second basic feature (ii) of the heartbeat model mentioned earlier. These points can be obtained easily by considering the eigenvalue of the matrix **A** in Eq. (3)

$$\lambda_{1,2} = \frac{1}{2\varepsilon}\left(-\left(3x_1^2 - T\right) \pm \sqrt{\left(3x_1^2 - T\right)^2 - 4\varepsilon}\right). \tag{4}$$

The condition that the real part of the eigenvalues is negative is $3x_1^2 - T > 0$. Therefore, the system is stable if $x_1 \geq \sqrt{T/3}$ which refers to the section AB, and $x_1 \leq -\sqrt{T/3}$ which describes the section CD. In other words, the thresholds for switching between the diastolic and the systolic states at point B is $x_1 = \sqrt{T/3}$, and $x_1 = -\sqrt{T/3}$ at point C.

The stable equilibrium point that represents the state of diastole can be determined by changing the value of x_d in Eq. (2) such that it satisfies the stability condition above. Fig. 2 displays the phase portrait of the system with x_d = 1.024. The equilibrium point is stable at (1.024, -0.0497), and qualifies to be the diastolic equilibrium state, that is, satisfies the first feature (i): a stable equilibrium.

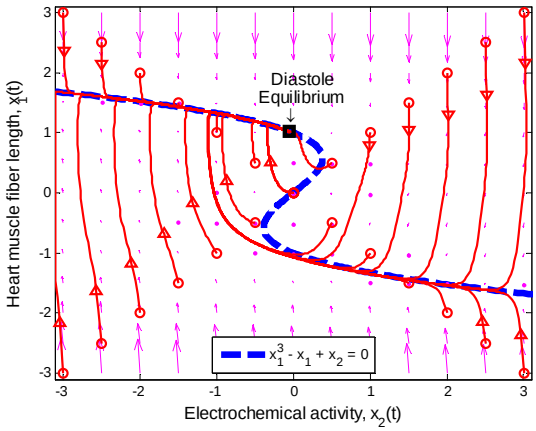

Figure 2. Phase portrait of the 2nd-order heartbeat system during diastole.

In Fig. 2, all of the trajectories, regardless of their initial conditions, end up at the diastolic equilibrium point. Since the equilibrium point is stable, the system will stay at this point forever unless there is an external excitation that forces the system to a new equilibrium point. In [8], the authors suggest modifying the system by adding a control input $u(t)$ as

$$\varepsilon \dot{x}_1 = -\left(x_1^3 - Tx_1 + x_2\right), \qquad T > 0, \tag{5}$$

$$\dot{x}_2 = \left(x_1 - x_d\right) + \left(x_d - x_s\right)u, \tag{6}$$

where the additional parameter x_s represents a typical fiber length when the heart is in the systolic state, and $u(t)$ represents cardiac pacemaker control mechanism that directs the heart into the diastolic and the systolic states. By proposing the cardiac pacemaker control signal $u(t)$ in the form of 0 and 1 (on-off control), the equilibrium point of the system can be changed between the diastolic and the systolic states.

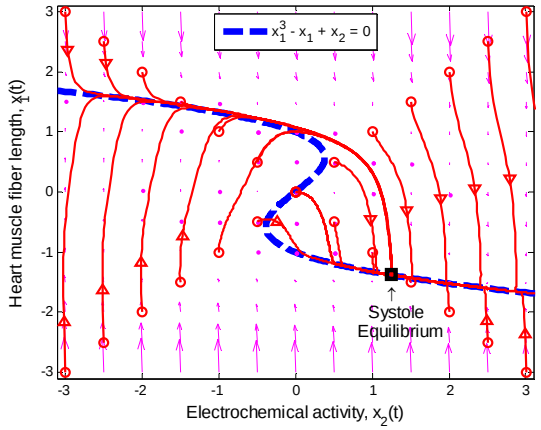

Figure 3. Phase portrait of the 2nd-order heartbeat system during systole.

Fig. 3 displays the phase portrait of Eqs. (5) and (6) with $u(t) = 1$, and $x_s = -1.3804$. The stable equilibrium point is located at (-1.3804, 1.25). Therefore, the on-off control scheme is successful in modeling the state changes from diastole to systole depending on the control signal.

Third-Order Nonlinear Heartbeat Model

The 3rd-order nonlinear heartbeat model is given by [2]

$$\varepsilon \dot{x}_1 = -\left(x_1^3 + x_1 x_2 + x_3\right), \tag{7}$$

$$\dot{x}_2 = -2x_1 - 2x_2, \tag{8}$$

$$\dot{x}_3 = -x_2 - 1 + u, \tag{9}$$

where $x_1(t)$ represents the length of the muscle fiber, $x_2(t)$ represents tension in the muscle fiber, $x_3(t)$ is related to electrochemical activity, ε is a small positive constant, and $u(t)$ represents cardiac pacemaker control signal which directs the heart into the diastolic and the systolic states.

The dynamics of the 3rd-order system is similar to that of the 2nd-order system except that the dynamics of the muscle fiber tension is taken into consideration. In the 2nd-order system, this quantity is considered as a constant parameter.

In this paper, we will attempt to generate artificial or synthetic ECG signals by using the nonlinear feedback control strategy – input-output feedback linearization technique and methodology, to control the 2nd-order heartbeat model given by Eqs. (5) - (6), and the 3rd-order heartbeat model given by Eqs. (7) - (9).

3. NONLINEAR FEEDBACK LINEARIZATION

Consider a control-affine single-input single-output (SISO) nonlinear system described by

$$\dot{\mathbf{x}} = \mathbf{f}(\mathbf{x}) + \mathbf{g}(\mathbf{x})u\,, \qquad \mathbf{f}, \mathbf{g} : D \subset \mathbb{R}^n \to \mathbb{R}^n\,, \tag{10}$$

$$y = h(\mathbf{x})\,, \qquad h : D \subset \mathbb{R}^n \to \mathbb{R}\,, \tag{11}$$

where $\mathbf{x} \in \mathbb{R}^n$ is the state vector, $u, y \in \mathbb{R}$ are the control and output signals, respectively; $\mathbf{f}$, $\mathbf{g}$ are smooth vector fields in a domain D and h a smooth function in D, where D is an open set in $\mathbb{R}^n$.

Given the nonlinear system of Eq. (10) and the measurement of Eq. (11), our goal is to find a *diffeomorphism* or nonlinear transformation of the form $\mathbf{z} = \mathbf{T}(\mathbf{x})$ with $\mathbf{T}(\mathbf{0}) = \mathbf{0}$ that transforms the nonlinear system in the *x-coordinates* to a linear system in the *z-coordinates.* One of the most important reasons for finding the transformation is that the powerful linear system theory and methodologies can be applied once a nonlinear system has been linearized.

Differentiating the output $y(t)$ with respect to t yields

$$\dot{y} = L_{\mathbf{f}}h(\mathbf{x}) + L_{\mathbf{g}}h(\mathbf{x})u\,, \tag{12}$$

where $L_{\mathbf{f}}h(\mathbf{x})$ and $L_{\mathbf{g}}h(\mathbf{x})$ denote the Lie derivatives of $h(\mathbf{x})$ with respect to $\mathbf{f}(\mathbf{x})$ and $\mathbf{g}(\mathbf{x})$, respectively. If $L_{\mathbf{g}}h(\mathbf{x}) = 0$, then $\dot{y}(t)$ is independent of $u(t)$. Continuing successive differentiation ρ times until $u(t)$ appears explicitly, we obtain

$$y^{(\rho)} = \underbrace{L_{\mathbf{f}}^{\rho}h(\mathbf{x})}_{b(\mathbf{x})} + \underbrace{L_{\mathbf{g}}L_{\mathbf{f}}^{\rho-1}h(\mathbf{x})}_{D(\mathbf{x})}\,u\,. \tag{13}$$

The smallest integer ρ for which $u(t)$ appears is referred to as the *relative degree*. The nonlinear system in Eqs. (10) - (11) is said to have a well-defined relative degree ρ in a region $D_0 \subset D$ if

$$L_{\mathbf{g}}L_{\mathbf{f}}^{k}h(\mathbf{x}) = 0 \quad \forall k,\ 0 \le k < \rho - 1;\ \text{and}\ L_{\mathbf{g}}L_{\mathbf{f}}^{\rho-1}h(\mathbf{x}) \ne 0, \tag{14}$$

for all $\mathbf{x} \in D_0$. Note that $\rho \le n$. From Eq. (13), define

$$v \triangleq y^{(\rho)} = b(\mathbf{x}) + D(\mathbf{x})\,u\,, \tag{15}$$

where $v(t)$ is a one-dimensional *transformed input* created by the feedback linearization process; $b(\mathbf{x})$ is called the *nonlinearity cancellation factor*, and $D(\mathbf{x})$ the *decoupling matrix* (a scalar in the present SISO system). Equation (15) yields the linearizing feedback control law [10 – 12]:

$$u = D^{-1}(\mathbf{x})\left(-b(\mathbf{x}) + v\right), \tag{16}$$

provided $D(\mathbf{x})$ is nonsingular (invertible).

To develop an overall representation of the system for the case with relative degree $\rho < n$, the diffeomorphism $\mathbf{z} = \mathbf{T}(\mathbf{x})$ can be expressed as

$$\mathbf{z} = \mathbf{T}(\mathbf{x}) \triangleq \left[\begin{array}{c} \boldsymbol{\xi} \\ \hline \boldsymbol{\eta} \end{array}\right] = \left[\begin{array}{c} h(\mathbf{x}) \\ \vdots \\ L_{\mathbf{f}}^{\rho-1} h(\mathbf{x}) \\ \hline \phi_1(\mathbf{x}) \\ \vdots \\ \phi_{n-\rho}(\mathbf{x}) \end{array}\right], \tag{17}$$

where $\boldsymbol{\xi} \in \mathbb{R}^{\rho}$, $\boldsymbol{\eta} \in \mathbb{R}^{n-\rho}$; and $\phi_i(\mathbf{x})$, $i = 1,...,n-\rho$ are chosen such that $\mathbf{T}(\mathbf{x})$ is a diffeomorphism on a domain $D_0 \subset D$, that is, the Jacobian matrix associated with $\mathbf{T}(\mathbf{x})$ is nonsingular, and

$$L_{\mathbf{g}} \phi_i(\mathbf{x}) = \frac{\partial \phi_i}{\partial \mathbf{x}} \mathbf{g}(\mathbf{x}) = 0, \quad 1 \le i \le n-\rho, \tag{18}$$

for all $\mathbf{x} \in D_0$.

The diffeomorphism in Eq. (17) leads to the *normal form*

$$\dot{\boldsymbol{\xi}} = \mathbf{A}_{\xi} \boldsymbol{\xi} + \mathbf{B}_{\xi} v, \tag{19}$$

$$\dot{\boldsymbol{\eta}} = \mathbf{f}_{\mathbf{0}}(\boldsymbol{\xi}, \boldsymbol{\eta}), \tag{20}$$

$$y = h(\mathbf{x}) = \xi_1. \tag{21}$$

Setting $\boldsymbol{\xi}(t) = 0$ in Eq. (20) for all $t \ge 0$ yields

$$\dot{\boldsymbol{\eta}} = \mathbf{f}_{\mathbf{0}}(0, \boldsymbol{\eta}), \tag{22}$$

which represents the *zero dynamics* for Eqs. (10) and (11). The stability of the zero dynamics in Eq. (22) is an important issue in designing a controller. The system whose zero dynamics are asymptotically stable in the domain of interest is called a *minimum phase system*. The local asymptotic stability of the zero dynamics is, clearly, the necessary and sufficient conditions for the local asymptotic stability of the feedback linearized system in Eqs. (19) - (21) [12, 13]. In the case that the zero dynamics are unstable in the region of interest, the system is known as a *non-minimum phase system*. Generally, a system of this type cannot be used for state-feedback control system design because some of the state variables will diverge to infinity. In this case, the stabilization of the unstable zero dynamics need to be considered, if possible.

Asymptotic Output Tracking

Let the control objective be steering the output $y(t)$ to a desired reference $y_r(t)$. This gives rise to an output tracking control problem. Define the output tracking error as

$$e \triangleq y - y_r. \tag{23}$$

The main objective is to force $e(t) \to 0$ such that $y(t) \to y_r(t)$ as $t \to \infty$. It follows that

$$\left.\begin{array}{l} \dot{e} = \dot{y} - \dot{y}_r, \\ \quad \vdots \\ e^{(\rho)} = y^{(\rho)} - y_r^{(\rho)} = v - y_r^{(\rho)}. \end{array}\right\} \tag{24}$$

A suitable tracking control law for the transformed input $v(t)$ is given by

$$v = -\mathbf{K}_{\xi} \mathbf{e} + y_r^{(\rho)}, \tag{25}$$

where $\mathbf{e} = \left[\begin{array}{cccc} e & \dot{e} & \ddot{e} & \cdots & e^{(\rho-1)} \end{array}\right]^T$, and the constant feedback gain $\mathbf{K}_{\xi} \in \mathbb{R}^{1 \times \rho}$ is determined such that $\mathbf{A}_{cl} = \mathbf{A}_{\xi} - \mathbf{B}_{\xi} \mathbf{K}_{\xi}$ is Hurwitz, that is, all eigenvalues of $\mathbf{A}_{cl}$ lie in the open left-haft complex plane. Finally, the overall closed-loop nonlinear system in the *x*-coordinates is given by

$$\dot{\mathbf{x}} = \mathbf{f}(\mathbf{x}) + \mathbf{g}(\mathbf{x}) D^{-1}(\mathbf{x}) \left[-b(\mathbf{x}) + v\right], \tag{26}$$

where $v(t)$ is given by Eq. (25).

4. APPLICATION TO HEARTBEAT MODELS

Controlling the Second-Order Nonlinear Heartbeat System

Consider the 2nd-order nonlinear heartbeat model given by Eqs. (5) - (6). First, we consider choosing the output measurement to be $y(t) = x_2(t)$. This selection is reasonable in the physical viewpoint since the electrochemical activity can be measured as the potential across the membrane of the muscle fiber [2]. Differentiating $y(t)$ with respect to t yields

$$\dot{y} = x_1 - x_d + \left(x_d - x_s\right) u, \tag{27}$$

where $u(t)$ appears which shows that the relative degree is $\rho = 1$. Thus, the heartbeat system has both external and internal dynamics. The diffeomorphism is given by

$$\mathbf{z} = \mathbf{T}(\mathbf{x}) = \left[\begin{array}{c} h(\mathbf{x}) \\ \hline \phi(\mathbf{x}) \end{array}\right] = \left[\begin{array}{c} \xi \\ \hline \eta \end{array}\right] = \left[\begin{array}{c} x_2 \\ \hline x_1 \end{array}\right]. \tag{28}$$

The Jacobian matrix associated with $\mathbf{T}(\mathbf{x})$ is given by

$$\frac{\partial \mathbf{T}(\mathbf{x})}{\partial \mathbf{x}} = \left[\begin{array}{cc} 0 & 1 \\ 1 & 0 \end{array}\right], \tag{29}$$

which is nonsingular for all $\mathbf{x} \in \mathbb{R}^2$; therefore $\mathbf{T}(\mathbf{x})$ is a global diffeomorphism for Eqs. (5) and (6). Equation (28) shows that the original system is already in a normal form when the output is chosen as $y(t) = x_2(t)$. However, one of the benefits of deriving (28) is that it reveals $x_1(t)$ as the internal dynamics and $x_2(t)$ as the external dynamics of the system. The resulting system in normal form is obtained as

$$\dot{\xi} = \eta - x_d + \left(x_d - x_s\right) u, \tag{30}$$

$$\dot{\eta} = -\frac{1}{\varepsilon}\left(\eta^3 - T\eta + \xi\right), \tag{31}$$

$$y = \xi. \tag{32}$$

Next, consider the stability of the internal dynamics in Eq. (31). The zero dynamics satisfy

$$\dot{\eta} = f_0(\xi,\eta)\big|_{\xi=0} = -\frac{1}{\varepsilon}\left(\eta^3 - T\eta\right). \tag{33}$$

There are three equilibrium points for Eq. (33): $\eta = 0$, $\pm\sqrt{T}$. We applied the Lyapunov indirect stability theorem [10] to analyze the stability of the equilibrium points. First, at the origin

$$\lambda_1 = -\frac{1}{\varepsilon}\left(3\eta^2 - T\right)\Big|_{\eta=0} = \frac{T}{\varepsilon}. \tag{34}$$

Since T and ε are positive constants, it follows that $\lambda_1 > 0$; hence the equilibrium at the origin is unstable. Consider the other equilibrium points

$$\lambda_{2,3} = -\frac{1}{\varepsilon}\left(3\eta^2 - T\right)\Big|_{\eta=\pm\sqrt{T}} = -2\frac{T}{\varepsilon}. \tag{35}$$

It is clear that $\lambda_2 < 0$ and $\lambda_3 < 0$ for all $T > 0$ and $\varepsilon > 0$, thus the equilibrium points at $\eta = \pm\sqrt{T}$ are asymptotically stable. In other words, regardless of the unstable equilibrium at the origin, the steady-state of the zero dynamics will end up at either the point $\eta = \sqrt{T}$ or $\eta = -\sqrt{T}$ depending on the initial condition. As a result, the zero dynamics are asymptotically stable. We conclude that the system is a minimum-phase system.

To proceed to the output tracking control design task, define the tracking error as $e \triangleq y - y_r$, where $y_r(t)$ is the reference input. It follows that

$$\dot{e} = x_1 - x_d + \left(x_d - x_s\right)u - \dot{y}_r \triangleq v - \dot{y}_r. \tag{36}$$

where $v(t)$ is the transformed input. Let the tracking control law for the transformed input $v(t)$ be given by

$$v = -Ke + \dot{y}_r = -K\left(x_2 - y_r\right) + \dot{y}_r, \tag{37}$$

where $K = 100$ is obtained by placing the real pole at -100 of the complex plane. We obtain the resulting linearizing feedback control law

$$u = \frac{1}{x_d - x_s}\left[-K\left(x_2 - y_r\right) + \dot{y}_r - \left(x_1 - x_d\right)\right]. \tag{38}$$

Finally, substituting Eq. (38) into Eqs. (5) - (6), and using Eq. (26) yields the overall feedback control system in the *x*-coordinates

$$\varepsilon\dot{x}_1 = -\left(x_1^3 - Tx_1 + x_2\right), \qquad T > 0, \tag{39}$$

$$\dot{x}_2 = -K\left(x_2 - y_r\right) + \dot{y}_r, \tag{40}$$

$$y = x_2. \tag{41}$$

Fig. 4 to 6 show the results of tracking real discrete ECG data obtained from the PhysioNet database [14]. In Fig. 4, the initial condition of $x_1(0)$ is 0.01 and the steady state converges to $\sqrt{T} = 1$ as expected. The output $x_2(t)$ tracks the discrete ECG data very nicely as shown in Fig. 5. The control signal or pacemaker in Eq. (38) which is used to generate and to track the ECG signal is shown in Fig. 6.

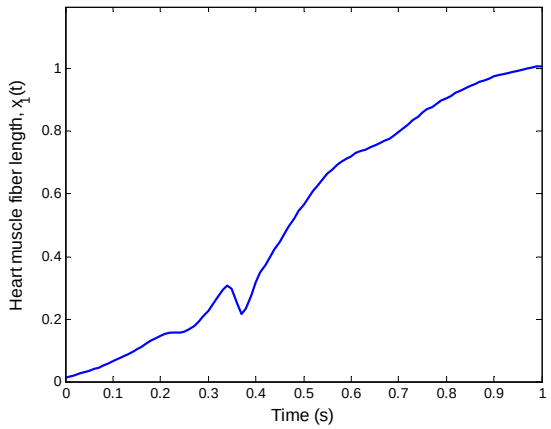

Figure 4. Simulation result of $x_1(t)$ of the 2nd-order heartbeat system.

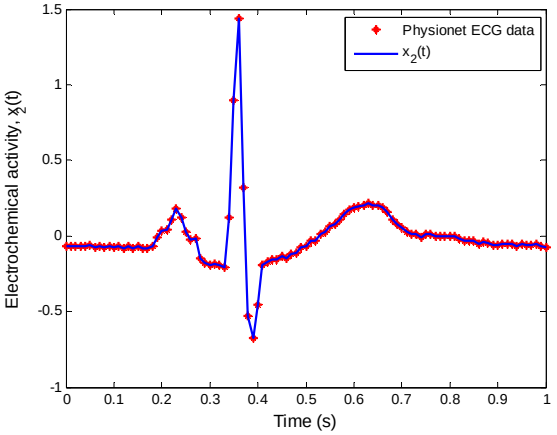

Figure 5. Simulation result of $x_2(t)$ of the 2nd-order heartbeat system.

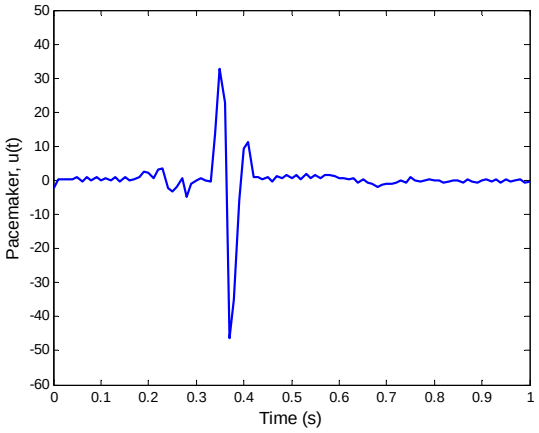

Figure 6. Simulation result of $u(t)$ of the 2nd-order heartbeat system.

Controlling the Third-Order Nonlinear Heartbeat System

Consider the 3rd-order heartbeat system given by Eqs. (7) - (9), and choosing the output as $y(t) = x_3(t)$. Differentiating the output with respect to *t* yields

$$\dot{y} = -x_2 - 1 + u, \tag{42}$$

which shows that the relative degree is $\rho = 1$. The diffeomorphism is obtained as

$$\mathbf{z} = \mathbf{T}(\mathbf{x}) = \begin{bmatrix} h(\mathbf{x}) \\ \phi_1(\mathbf{x}) \\ \phi_2(\mathbf{x}) \end{bmatrix} = \begin{bmatrix} \xi \\ \eta_1 \\ \eta_2 \end{bmatrix} = \begin{bmatrix} x_3 \\ x_1 \\ x_2 \end{bmatrix}. \tag{43}$$

It can be shown easily that the Jacobian matrix associated with $\mathbf{T}(\mathbf{x})$ is nonsingular for all $\mathbf{x} \in \mathbb{R}^3$; thus $\mathbf{T}(\mathbf{x})$ is a global diffeomorphism for Eqs. (7) - (9). The resulting system in normal form is described by

$$\dot{\xi} = -\eta_2 - 1 + u, \tag{44}$$

$$\dot{\eta}_1 = -\frac{1}{\varepsilon}\left(\eta_1^3 + \eta_1\eta_2 + \xi\right), \tag{45}$$

$$\dot{\eta}_2 = -2\eta_1 - 2\eta_2, \tag{46}$$

$$y = \xi. \tag{47}$$

The zero dynamics are given by

$$\left.\begin{aligned} \dot{\eta}_1 &= -\frac{1}{\varepsilon}\left(\eta_1^3 + \eta_1\eta_2\right), \\ \dot{\eta}_2 &= -2\eta_1 - 2\eta_2. \end{aligned}\right\} \tag{48}$$

There are two equilibrium points associated with Eq. (48): the origin and $(\eta_1, \eta_2) = (1, -1)$. Applying the Lyapunov indirect stability theorem [10] to analyze the stability of each equilibrium point yields

$$\mathbf{A}_1 = \begin{bmatrix} -\frac{1}{\varepsilon}\left(3\eta_1^2 + \eta_2\right) & -\frac{1}{\varepsilon}\eta_1 \\ -2 & -2 \end{bmatrix}_{(1,-1)} = \begin{bmatrix} -\frac{2}{\varepsilon} & -\frac{1}{\varepsilon} \\ -2 & -2 \end{bmatrix}. \tag{49}$$

It follows that $\mathrm{Re}(\lambda_i) < 0,\ \forall i = 1, 2$; where λ represents the eigenvalue. Therefore, the matrix $\mathbf{A}_1$ is Hurwitz and the equilibrium point at (1,-1) is asymptotically stable.

Next, consider the equilibrium point at the origin

$$\mathbf{A}_2 = \begin{bmatrix} -\frac{1}{\varepsilon}\left(3\eta_1^2 + \eta_2\right) & -\frac{1}{\varepsilon}\eta_1 \\ -2 & -2 \end{bmatrix}_{(0,0)} = \begin{bmatrix} 0 & 0 \\ -2 & -2 \end{bmatrix}. \tag{50}$$

The eigenvalues of $\mathbf{A}_2$ are 0 and -2. Since one of the eigenvalue is zero, we cannot draw the stability conclusion by the Lyapunov indirect theorem. However, using the *reduced system theorem* [10], it can be shown that the zero dynamics in Eq. (48) are asymptotically stable. This conclusion is illustrated by the phase portrait of the zero dynamics itself as shown in Fig. 7. All trajectories with initial conditions $\eta_1 \geq 0$ converge to the origin. With the stability analysis results, we conclude that the normal form system in Eqs. (44) - (47) is a minimum-phase system.

To proceed on the output tracking control design task, define the tracking error as $e \triangleq y - y_r$ where $y_r(t)$ is the reference input. It follows that

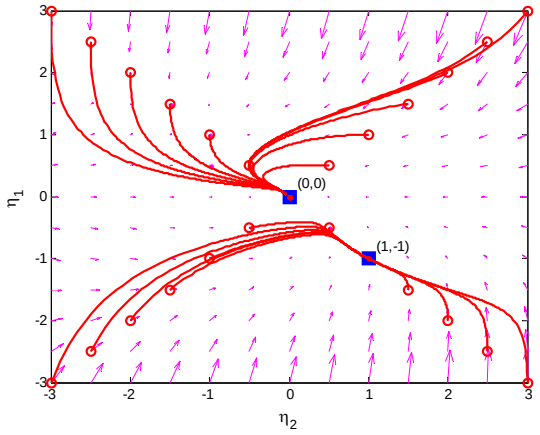

Figure 7. Phase portrait of zero dynamics.

$$\dot{e} = \dot{x}_3 - \dot{y}_r = -x_2 - 1 + u - \dot{y}_r \triangleq v - \dot{y}_r, \tag{51}$$

where $v(t)$ is the transformed input. Let the tracking control law for the transformed input $v(t)$ be given by

$$v = -Ke + \dot{y}_r = -K\left(x_3 - y_r\right) + \dot{y}_r, \tag{52}$$

where $K = 100$ is obtained by placing the real pole at -100. The resulting linearizing feedback control law is obtained as

$$u = -K\left(x_3 - y_r\right) + \dot{y}_r + x_2 + 1. \tag{53}$$

The simulation results for the final feedback control system in the *x*-coordinates are shown in Fig. 8-11. The state trajectories of the muscle fiber length $x_1(t)$ and the muscle fiber tension $x_2(t)$ are displayed in Fig. 8 and 9, respectively. Fig. 10 demonstrates the result of the output $y(t) = x_3(t)$ that tracks the ECG data obtained from the William Beaumont Hospitals. Fig. 11 illustrates the pacemaker of Eq. (53) used to generate the results of the 3rd-order heartbeat control system.

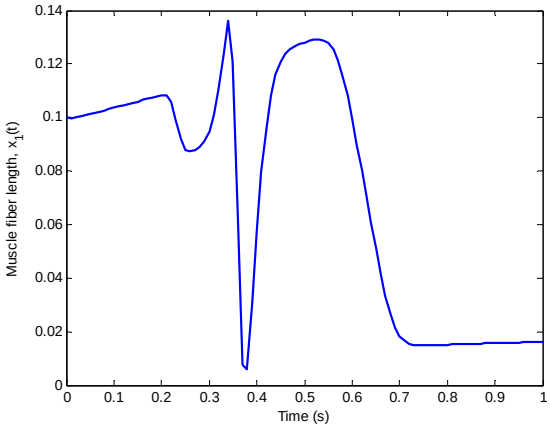

Figure 8. Simulation result of $x_1(t)$ of the 3rd-order heartbeat system.

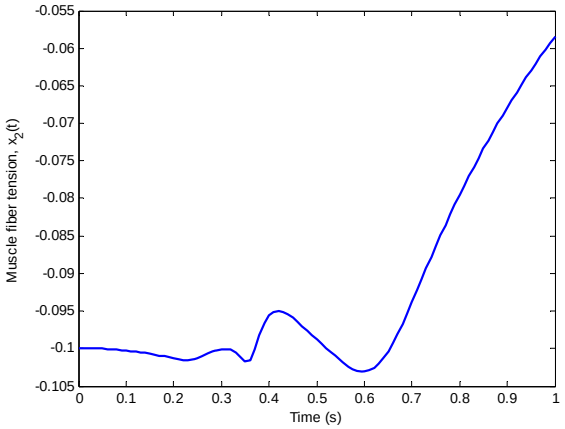

Figure 9. Simulation result of $x_2(t)$ of the 3rd-order heartbeat system.

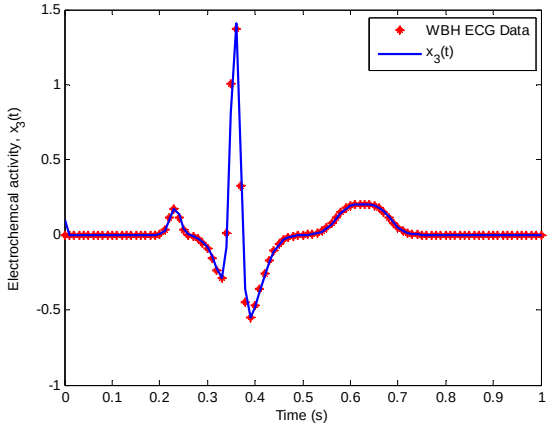

Figure 9. Simulation result of $x_3(t)$ of the 3rd-order heartbeat system.

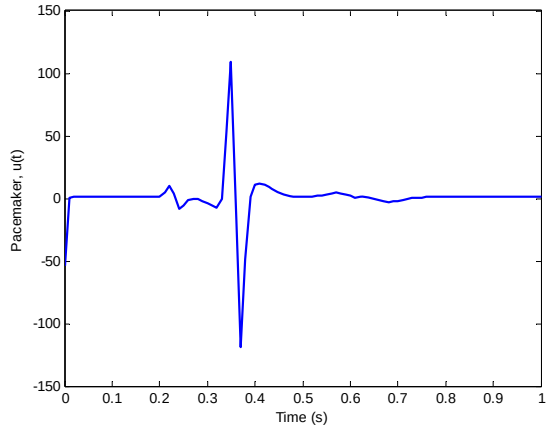

Figure 11. Simulation result of $u(t)$ of the 3rd-order heartbeat system.

5. CONCLUSION

We presented the application of nonlinear control system theory based on input-output feedback linearization to biological heartbeat systems. Several cardiac related mathematical models have been investigated and two models developed by Zeeman were chosen in this study. The models were modified by adding a control input into the system, thereby creating two interesting control-affine SISO nonlinear systems. We showed that the resulting heartbeat models are minimum-phase systems suitable for the design of output tracking control laws; these output tracking control laws were used to generate synthetic ECG signals. The simulation results show that the systems can be forced to track the ECG data obtained from the William Beaumont Hospitals and the PhysioNet database [14] satisfactorily. Other biomedical applications of Zeeman's models using the nonlinear control technique developed in this paper are under consideration.

ACKNOWLEDGMENT

This research was supported by Oakland University-Beaumont Multidisciplinary Research Award under fund #39709. We would also like to thank Dr. Robert Hammond of the William Beaumont Hospitals, Royal Oak, Michigan for providing a set of ECG data used in the simulation studies.

REFERENCES

[1] N. Kannathal, C. M. Lim, U. Rajendra Acharya, and P. K. Sadasivan, "Cardiac state diagnosis using adaptive neuro-fuzzy technique", **Medical Engineering & Physics**, Vol. 28, 2006, pp. 809-815.

[2] E. C. Zeeman, "Differential equations for the heartbeat and nerve impulse", **Towards a Theoretical Biology**, Vol. 4, 1972, pp. 8-67.

[3] F. A. Roberge, P. Bhereur, and R. A. Nadeau, "A cardiac pacemaker model", **Medical & Biology Engineering**, Vol. 9, 1971, pp. 3-12.

[4] D. S. Breitenstein, "Cardiovascular modeling: the mathematical expression of blood circulation", Master's thesis, University of Pittsburgh, PA, 1993.

[5] Y. C. Yu, J. Boston, M. Simaan, and J. Antaki, "Estimation of systemic vascular bed parameters for artificial heart control", **IEEE Transactions on Automatic Control**, Vol. 43, June 1998, pp. 765-777.

[6] A. Ferreira, S. Chen, M. Simaan, J. Boston, and J. Antaki, "A nonlinear state-space model of a combined cardiovascular system and a rotary pump", **Proceedings of the 44th IEEE Conference on Decision and Control, and the European Control conference 2005**, Seville, Spain, 2005.

[7] N. Jafarnia-Dabanloo, D. C. McLernon, H. Zhang, A. Ayatollahi, and V. Johari-Majd, "A modified Zeeman model for producing HRV signals and its application to ECG signal generation", **Journal of Theoretical Biology**, Vol. 244, 2007, pp. 180-189.

[8] D. S. Jones and B. D. Sleeman, **Differential Equations and Mathematical Biology**, Chapman & Hall/CRC, UK, 2003.

[9] P. E. McSharry, G. D. Clifford, L. Tarassenko and L. A. Smith, "A Dynamical Model for Generating Synthetic Electrocardiogram Signals", **IEEE Transactions on Biomedical Engineering**, Vol. 50, No. 3, March 2003, pp. 289-294.

[10] H. K. Khalil, **Nonlinear Systems**, 3rd edition, New Jersey: Prentice Hall, 2002.

[11] A. Isidori, **Nonlinear Control Systems**, New York: Springer-Verlag, 1995.

[12] M. A. Henson and D. E. Seborg, **Nonlinear Process Control**, New Jersey: Prentice Hall, 1997.

[13] C. I. Byrnes and A. Isidori, "Asymptotic Stabilization of Minimum Phase Nonlinear Systems", **IEEE Transaction on Automatic Control**, Vol. 36, No. 10, October 1991, pp. 1122-1137.

[14] A. L. Goldberger, L. A. N. Amaral, L. Glass, J. M. Hausdorff, P. Ch. Ivanov, R. G. Mark, J. E. Mietus, G. B. Moody, C. K. Peng, H. E. Stanley, "PhysioBank, PhysioToolkit, and PhysioNet: Components of a New Research Resource for Complex Physiologic Signals", **Circulation**, Vol. 101, No. 23, pp. e215-e220, 2000.